JOURNAL OF PROPULSION AND POWER
Vol. 11, No. 4, July–August 1995

HMX and RDX: Combustion Mechanism and Influence on Modern Double-Base Propellant Combustion

Anatoli Zenin*
Russian Academy of Sciences, Moscow, Russia

Experimental investigations of the burning wave structures of HMX and RDX were carried out by microthermocouple technique at a pressure of 1–70 (90) atm. Burning-surface temperature, heat release in solid, heat feedback from gas to solid, and heat-release rate in gas near the surface were obtained. The data obtained show that in the condensed phase of combustion waves of nitramines, evaporation, and thermal decomposition occur simultaneously, with heat release in the solid being negative at $p < 5$–10 atm and positive at $p > 5$–10 atm. Activation energies of HMX and RDX decomposition in combustion waves were evaluated. Published results of investigations of the thermal burning wave structures of double-base propellants (DBP) containing HMX and various catalysts were used to establish the influence of additional nitramines on the unified dependencies of simple DBPs. It was found that the gasification law, heat-release law in the solid, and heat-feedback law do not change, but that the dark zone laws and dependencies for temperature sensitivities change significantly when HMX is added.

Nomenclature

c, c_0, c_p = specific heats of condensed and gas phases, respectively, cal/g K
E = activation energy in solid, kcal/mole
k, k_I = thermal conductivities of condensed and gas phases, cal/cm s K
k_{01} = pre-exponential multiplier, 1/s
$\bar{k}_1$, $\bar{k}_0$ = coefficients of gas emissivity and solid absorption
L = dark zone thickness, mm
l, l_m = thicknesses of thermal layer and melted layer in condensed phase, μm
m, r_b = mass and linear burning rate, g/cm^{2}s and cm/s
p = pressure, atm
Q, Q_v = heat release in solid and caloric power (heat of explosion) of propellant at constant volume, cal/g
Q^* = maximum heat release in solid, cal/g
q, q_r = heat feedback from gas to burning surface by heat conduction and radiation, cal/g
q_m = heat of melting, cal/g
r = temperature sensitivity of burning surface temperature at constant pressure, $(\partial T_s/\partial T_0)_p$
T_s, T_1, T_f = temperatures of burning surface, dark zone, and flame, °C
$T(x)$ = temperature distribution in combustion wave, °C
T_0, T_m = initial temperature of sample and melting temperature, °C
x = distance, mm
β = temperature sensitivity of burn rate at constant pressure, $(\partial \ln m/\partial T_0)_p$, 1/K
ρ, ρ_g = solid density and gas density, g/cm^3
τ_r = residence time, ms
Φ_0 = heat release rate in gas near burning surface, kcal/cm^{3}s
ϕ = temperature gradient in gas at surface, $(dT/dx)_0$, K/cm
χ = thermal diffusivity of condensed phase, cm^2/s

Received Dec. 1, 1994; revision received Feb. 16, 1995; accepted for publication March 8, 1995.
*Professor, Institute of Chemical Physics.

Introduction

THE use of cyclic nitramines HMX and RDX offers many advantages: high energy; large amount of gas; high values of specific impulse for rocket propellants; and nontoxic, nonsmoky, and noncorrosive exhaust products. A great deal of work has been devoted to investigating the combustion mechanism of the nitramines and the systems into which they are incorporated. Data on the decomposition, pyrolysis, deflagration, and macrokinetic parameters of HMX and RDX are given in Ref. 1. The burning-rate behavior of composite propellant systems with HMX and RDX was investigated in Refs. 2–11. The incorporation of nitramines into composite propellants and the increase of nitramine content generally leads to a decrease in the burning rate; different binders can radically alter the morphology of the burning surface and thereby change the combustion mechanism. The problems of catalysts in such systems and the influence of meltability of the oxidizer and binder on the catalytic effect have also received a good deal of attention.

The first objective of this work is to experimentally investigate the thermal wave structures of HMX and RDX as monopropellants. The results obtained (some of which are presented in Refs. 12 and 13) provide answers to some of the questions about the mechanism of nitramine combustion. The difficulty of finding effective catalysts for nitramine-based propellants is well-known. One way of solving the problem is to use components of double-base propellants (DBP), which are more sensitive to catalytic influence.[2,14] The second phase of the present work is devoted to the experimental investigation of the thermal burning wave structure of modern propellants containing components of DBP, different values of HMX, and different catalysts. Some of the results are presented in Refs. 15 and 16. The experimental data obtained are analyzed by means of the unified empirical dependencies for combustion wave parameters of simple DBP.[17,18] Plotting the data obtained for modern complex propellants on the curves of dependencies provides an insight into the combustion mechanism by establishing the coincidences and discrepancies between the obtained data. Comparison with the data obtained for HMX and RDX gives additional information about the mechanism of complex propellant combustion. Experimental results were achieved mainly by means of a microthermocouple technique described in the second section. The third portion of the present work contains the results and a discussion of the mechanism of combustion of HMX and

RDX. The fourth section contains the results of investigations of complex propellants with nitramines and catalysts and a discussion of their combustion mechanisms.

Methods of Investigations

Experimental investigations were performed mainly by a microthermocouple technique.[19] The idea of obtaining temperature profiles of combustion waves of propellants by microthermocouples was proposed in Refs. 20 and 21. However, tests instituted as a check upon measurements of the angle-shaped thermocouples used in Refs. 20 and 21 revealed that the thermocouples lose too much heat into the wires. U-shaped thermocouples and the criteria for their use in combustion waves of solid were then suggested.[19,22,23] The procedure of temperature curve corrections, methods of burning surface temperature registrations, and methods of elucidating information from temperature profiles were developed.[17,19,24] The validity of the analyses in a one-dimensional approximation was demonstrated in Refs. 17 and 19. Heat flux by conduction from gas into solid in stable combustion waves can be obtained by the slope of the temperature profile near the burning surface

$$qm = k_1(T)\left(\frac{dT}{dx}\right)_0$$

Heat feedback from gas into solid takes the form of

$$q = k_1(T)\phi/m \tag{1}$$

Heat release in a solid is

$$Q = c(T_s - T_0) - q - q_r + q_m \tag{2}$$

The heat conduction equation for a stable combustion wave is

$$(kT_x)_x - mc_pT_x + \Phi(T) = 0 \tag{3}$$

The profiles of volumetric heat-release rate $\Phi(T)$ in the gas phase can be obtained through temperature profiles and Eq. (3) by means of a special procedure.[17,19,25] Unified dependencies for parameters T_s, q, Q, and functions of $\Phi(T)$ were obtained in Refs. 17, 19, and 26 for simple DBP (without sufficient additions).

Burning Wave Structure and Combustion Mechanism of HMX and RDX

Temperature profiles $T(x)$ and surface temperatures T_s of steady combustion waves of HMX and of RDX have been

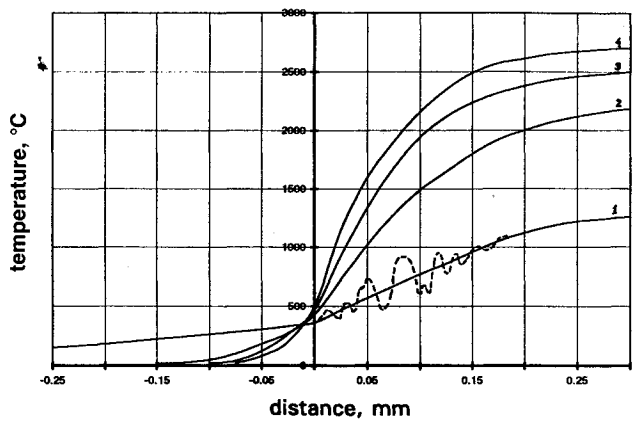

Fig. 1 Averaged temperature profiles $T(x)$ of HMX stable combustion waves. 1: 1, 2: 5, 3: 20, and 4: = 70 atm.

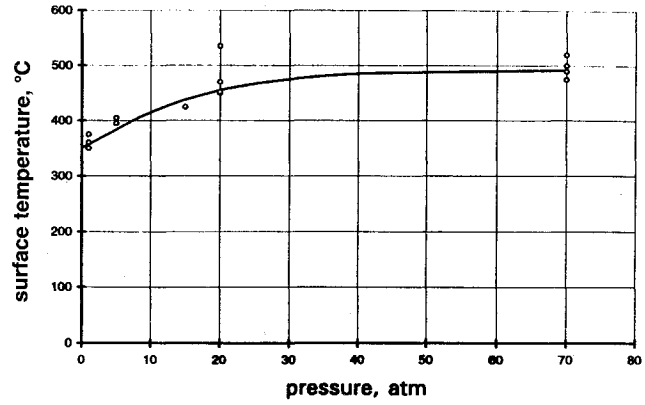

Fig. 2 Dependence of burning surface temperature T_s on pressure p; HMX.

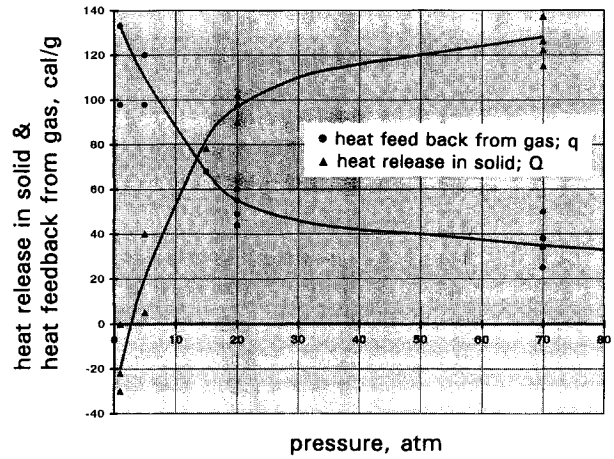

Fig. 3 Dependencies of heat release in solid Q and heat feedback by thermal conductivity from gas into solid q on pressure in combustion waves of HMX.

obtained at a pressure of 1-70 (90) atm in a nitrogen atmosphere. Initial temperature T_0 of the samples was 20°C. The samples were 12 mm long, 7 mm wide, and 5 mm high. U-shaped ribbon thermocouples made of alloys W + 5% Re and W + 20% Re and 3–5 μm thick, were imbedded into the samples when the samples were being pressed. Particles of the HMX and RDX powders were 20–50 μm in diameter. The density of HMX samples was 1.7 g/cm^3; and that of RDX samples was 1.66 g/cm^3.

HMX

Averaged temperature profiles obtained at 1, 5, 20, and 70 atm are shown in Fig. 1. Averagings were made by using five profiles determined for each pressure. When pressure increases, the temperature of the gas-phase gradient temperature and the flame temperature increases and the thermal layer l in solid narrows (l is determined as the thickness of the temperature decreasing e-times in solid). Since melting point T_m of solid HMX (T_m = 280°C) does not depend on pressure, the thickness of melting layer l_m can be determined by using $T(x)$ in a solid. Table 1 shows the dependencies of the obtained parameters on pressure, including dependence $l_m(p)$. Values of l_m are 2–3 times less than those of l; l_m decreases from 70 to 15 μm. Figure 2 shows dependence $T_s(p)$. It can be seen that averaged values of T_s increase from 360 to 490°C. Figure 3 depicts dependencies $q(p)$ and $Q(p)$. Note that averaged values of q decrease from 133 to 35 cal/g, and averaged values of Q increase from −11 to +128 cal/g when pressure increases from 1 to 70 atm. It was assumed that HMX melting heat was q_m = 28 cal/g; $q_r = \bar{k}_0\bar{k}_1\delta T_f^4/m$ where $\bar{k}_0$ = 0.1; $\bar{k}_1$ = 0.5; in solid c = 0.3 cal/g K, χ =

Table 1 HMX combustion wave parameters

p, atm	r_b, cm/s	m, g/cm²s	T_s, °C	$\Phi \times 10^{-4}$, K/cm	q, cal/g	Q, cal/g	l, μm	l_m, μm	Φ_0, Kcal/cm³s	T_f, °C	q_r, cal/g
1	0.035	0.06	360	4	133	−14	250	70	0.7	1600	11
5	0.15	0.255	400	14	110	+20	70	30	11	2300	12
20	0.4	0.68	460	18	53	+100	35	20	37	2600	7
70	1.0	1.7	490	30	35	+128	28	15	153	2750	6

Table 2 RDX combustion wave parameters

p, atm	r_b, cm/s	m, g/cm²s	T_s, °C	$\Phi \times 10^{-4}$, K/cm	q, cal/g	Q, cal/g	l, μm	l_m, μm	Φ_0, Kcal/cm³s	T_f, °C	q_r, cal/g
1	0.05	0.083	320	8	190	−84	170	120	2	1700	14
5	0.17	0.28	360	15	176	−61	50	25	13	2500	15
20	0.5	0.83	420	35	84	+58	35	20	87	2700	6
90	1.8	3.0	490	40	27	+140	25	15	360	2800	2

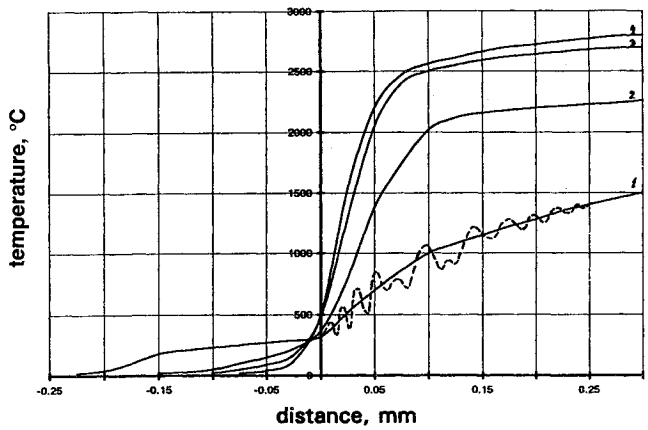

Fig. 4 Averaged temperature profiles $T(x)$ of RDX stable combustion waves. 1: 1, 2: 5, 3: 20, and 4: 90 atm.

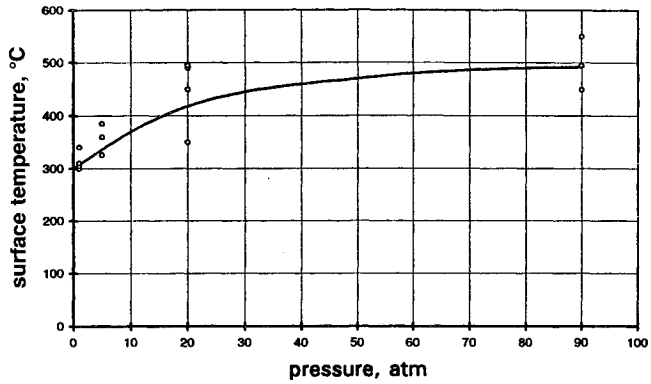

Fig. 5 Dependence of burning surface temperature T_s on pressure p; RDX.

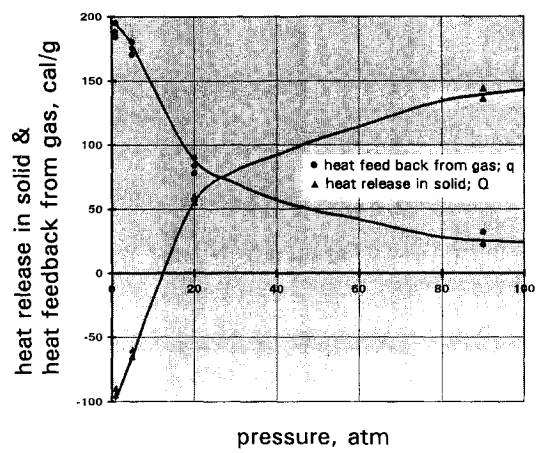

Fig. 6 Dependencies of heat release in solid Q and heat feedback by thermal conductivity from gas into solid q on pressure in combustion waves of RDX.

10^{-3} cm²/s; and in gas near surface $k_1 = 2 \times 10^{-4}$ cal/cm s K. Flame temperature T_f increases from 1900°C at 1 atm up to 2750°C at 70 atm.

At 1 atm the temperature of the gas phase near the surface pulsates (see dotted line in Fig. 1) due to occasional bursts of the bubbles formed in the melting zone. Many of the bubbles are 50–100 μm in diameter.[1]

The intensity of the gas-phase reaction close to the burning surface can be briefly outlined by the heat release rate Φ_0 estimated by the formula[17]:

$$\Phi_0 = c_p m \phi \qquad (4)$$

Table 1 shows that Φ_0 increases from 0.7 to 153 kcal/cm³s. The activation energy E of HMX decomposition in the combustion wave can be estimated by the formula: $m = A \cdot \exp(-E/2RT_s)$. It was established that $E = (46 \pm 2)$ Kcal/mole.

The data obtained show that two processes occur simultaneously in the condensed phase of HMX: evaporation and thermal decomposition. At low pressures ($p < 5$ atm), heat balance in the condensed phase is negative ($Q < 0$) since the heat absorption of the evaporation is greater than the heat release of the thermal decomposition; heat feedback from the gas phase compensates for the lack of heat. At elevated pressures, increased heat release of the thermal decomposition produces a positive heat balance.

RDX

Averaged temperature profiles obtained at 1, 5, 20, and 90 atm are presented in Fig. 4. Averaged burning-wave parameters are presented in Table 2. The obtained data show an increasing of surface temperature, gas-phase gradient temperature and flame temperature, and a narrowing of the thermal layer in solid. It is assumed that melting point of RDX $T_m = 200$°C. Table 2 shows that l_m occupies a significant part of l. Figure 5 shows dependence $T_s(p)$, and Fig. 6 shows dependencies $q(p)$ and $Q(p)$. From the figures and Table 2, one can see the increase of T_s from 320 to 490°C, the increase of Q from −84 to +140 cal/g, and the decrease of q from 190 to 27 cal/g, when pressure increases from 1 to 90 atm. It was assumed that all coefficients used for HMX are valid for RDX. The temperature pulsations observed at 1 atm (see dotted lines in Fig. 4) can be explained in the same way as for HMX. Activation energy has been estimated as equal to $E = (40 \pm 4)$ kcal/mole. The values of Φ_0 increase from 2 kcal/cm³s at 1 atm up to 360 kcal/cm³s at 90 atm. Flame temperature increases from 1700 to 2800°C.

Experimental results show that the same processes (evaporation and thermal decomposition) occur in the condensed phase of both RDX and HMX. However, the intensities of these processes are different. At pressures $p < 20$ atm the more intensive evaporation in RDX leads to a higher negative heat balance in the condensed phase ($Q = -84$ cal/g at 1 atm) and to a higher heat feedback from gas to solid ($q = 190$ cal/g at 1 atm). At elevated pressures, values of Q and q of RDX and HMX are almost the same, but the intensity of heat release in RDX is higher because m of RDX is higher. The gas-phase reaction rate near the surface is also higher for RDX than for HMX (compare Φ_0 in Tables 1 and 2).

Unified Dependencies for Wave Parameters of Propellants

The six empirical dependencies for burning-wave parameters of simple DBP [nitroglycerin (NG), nitrocellulose (NC), and various small additives] established in Refs. 17–19 and 26 are gasification law, heat release law in solid, heat feedback law from gas into solid, dark zone law, heat-release rate law, and temperature-profile law in gas at elevated pressures ($p > 100$ atm). The unified laws for the temperature sensitivities of combustion rate and surface temperature for simple DBP are suggested in Ref. 27. This section contains an analysis of the influence of catalysis and HMX additions on some of the dependencies. It is possible to cite evidence that the obtained unified dependencies point to the existence of chemical interaction between zones in the combustion waves of the substances investigated.

Gasification Law

The unified gasification law for simple DBP is illustrated in Fig. 7: see points no. 1, solid line (dashed lines represent confidence interval). Points no. 2 representing DBP with HMX additions (up to 30%) and points no. 3 representing DBP with different catalysts (including metal-organic catalysts) are also shown in Fig. 7. It can be seen that the gasification law for simple DBP is also practically valid for complex DBP with HMX and catalyst additions. The analytical form of the law is as follows[17,19]:

$$m = 1.8 \times 10^3 \exp(-5000/T_s) \tag{5}$$

where m has the unit of g/cm^{3}s. This dependence points to the existence of common macrokinetics for the limiting stage in the reaction layer of the condensed phase.[16,18] Indeed, the exact solution of heat conductivity equation for combustion waves is as follows[17,19]:

$$m^2 = \frac{k\rho}{Q^2}\frac{RT_s^2}{E} Q^* k_{01} \exp\left(-\frac{E}{RT_s}\right) \tag{6}$$

where $Q^* = 0.17Q_v$.

Plotting the experimentally obtained data for T_s, m, and Q on a chart in coordinates $\ln(mQ/T_s)$ vs T_s^{-1} shows the existence of the unified dependence that allows the values of E and k_{01} to be received [$E = (21 \pm 1)$ Kcal/mole, $k_{01} = (8^{+6}_{-2}) \times 10^{-9}$, 1/s].[17,19] Note that Eq. (5) is a simplified form of Eq. (6). It is important to stress the validity of Eq. (5) up to very high pressures.[19]

The data presented in Fig. 7 show that complex nitrates of ethers (NG and NC) are responsible for the limiting stage of the condensed-phase gasification of complex DBP with HMX and catalysts. It was noted also in Ref. 28 that the burning rate of mixtures with HMX and DB components is controlled by the DB components. Comparison of dependencies of $T_s(m)$ for HMX and complex DBP shows that values of T_s, for HMX are much higher than those for DBP (see Fig. 7). From the difference indicated in values of T_s, it follows that there is probably a mechanism of acceleration of nitramine gasification in the reaction layer of the condensed phase of complex DBP. It is perhaps, an evaporation-reinforced mechanism in the liquid layer of HMX. The mechanism can be responsible for the decreased burning rate of nitramine containing DBP since the additional evaporation requires some additional heat absorption in the reaction layer of the condensed phase. Experimental data in Refs. 14 and 15 show that, indeed, the introduction of HMX in DBP always significantly decreases the values of Q.

The unified gasification law in dimensionless form can be presented by the following equation:

$$\bar{m} = \exp(-\theta_s) \tag{7}$$

where $\bar{m} = m/m_{max}$, $m_{max} = 1.8 \times 10^3$ g/cm^{2}s is the maximum burning rate, and $\theta_s = E/RT_s$ is the reversal dimensionless surface temperature.

Heat-Release Law in Solid

Figure 8 represents the empirical dependence of the relative heat release in solid Q/Q_v on parameter $p/\sqrt{m}$ for the simple DBP (points no. 1), the DBP with different catalysts (points no. 2), and the DBP with HMX (points no. 3).

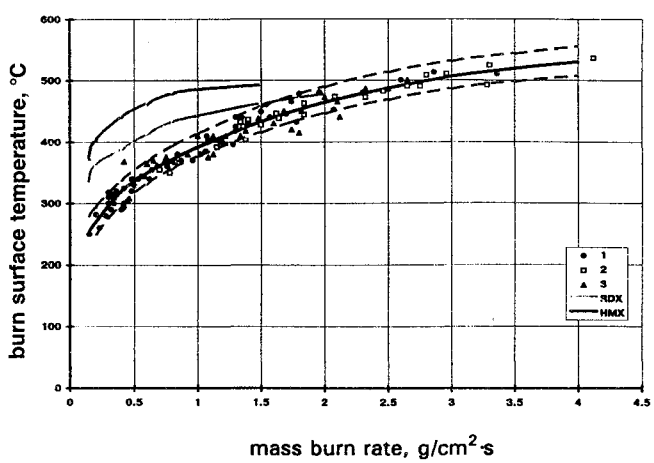

Fig. 7 Unified dependence $T_s(m)$ (gasification law) for simple double-base propellants (DBP), solid line. Dashed lines represent confidence interval. 1: points of simple DBP, 2: points of DBP + HMX (10–30%), and 3: points of DBP + strong catalysts. Comparison with dependencies $T_s(m)$ for HMX and RDX.

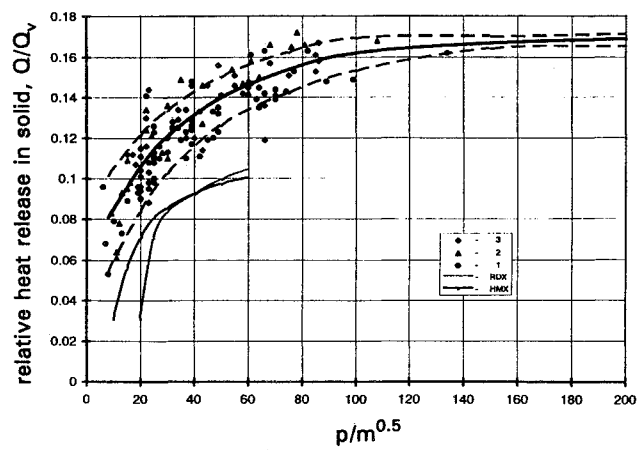

Fig. 8 Unified dependence $Q/Q_v(p/\sqrt{m})$ (heat release law in solid) for simple double-base propellants (DBP), solid line. Dashed lines represent confidence interval. 1: points of simple DBP, 2: point of DBP + strong catalysts, and 3: points of DBP + HMX (10–30%). Comparison with dependencies $Q/Q_v(p/\sqrt{m})$ for HMX and RDX.

The analytical form of the unified dependence (heat-release law in solid) for simple DBP presented in Refs. 17 and 26 is as follows:

$$Q/Q_v = 0.17 - 0.103 \times \exp(-0.0253p/\sqrt{m}) \quad (8)$$

where p has the unit of atm and m of g/cm^{2}s.

Points no. 2 and 3 were taken from Refs. 15 and 16. It can be seen that these points only increase scattering of experimental data and do not significantly change the position of the thick line represented by Eq. (8).

Placing Q/Q_v values of nitramines (see Tables 1 and 2) on Fig. 8 shows that nitramines have lower values of Q/Q_v than those of complex DBP, even in the range of positive values of Q of nitramines. These data confirm the decrease of Q in DBP when HMX is added, as indicated in Refs. 14 and 24.

Equation (8) shows that at high pressures $Q = 0.17Q_v = Q^*$. Obtained unified laws (5) and (8) allow us to calculate the heat balance of combustion waves of complex DBP by referring only to the external parameters m, p, and Q_v.

Heat-Feedback Law

The unified heat-feedback law from gas into solid can be represented by the equation:

$$q = c(T_s - T_0) - Q \quad (9)$$

Radiative heat feedback q_r is very small under the conditions investigated and can be neglected.

Dependencies for Temperature Sensitivities

Analysis shows that Eqs. (5) and (8) are valid for interval $-50 < T_0 < 50$°C. The following equations for temperature sensitivity of the burning rate $\beta = (\partial \ln m/\partial T_0)_p$, and for temperature sensitivity of the surface temperature $r = (\partial T_s/\partial T_0)_p$ can be obtained from Eqs. (5) and (8) by assuming that the dependence of q on T_0 is weak[27]:

$$\beta = [(2RT_s^2/E + 1.3 \times 10^{-3}pQ_v/c\sqrt{m})]^{-1} \quad (10)$$

$$r = [(1 + 1.3 \times 10^{-3}pQ_v/c\sqrt{m \times E/RT_s^2})] \quad (11)$$

The calculated parameters of β and r are in good agreement with the experimental values of β and r received for DBP without HMX (see Figs. 9 and 10). Calculations were made for the wide region of pressures and for interval 600 cal/g $< Q_v <$ 1180 cal/g. Note that Eqs. (10) and (11) present practically unified dependencies.

There is, however, a serious inconstancy between estimations by Eq. (10) and values of experimentally obtained β for DBP with HMX. Figure 11 shows that additions of HMX decrease β of complex DBP compared to the unified dependence (10). Decreasing β for mixtures containing DB components and HMX was reported in Ref. 28.

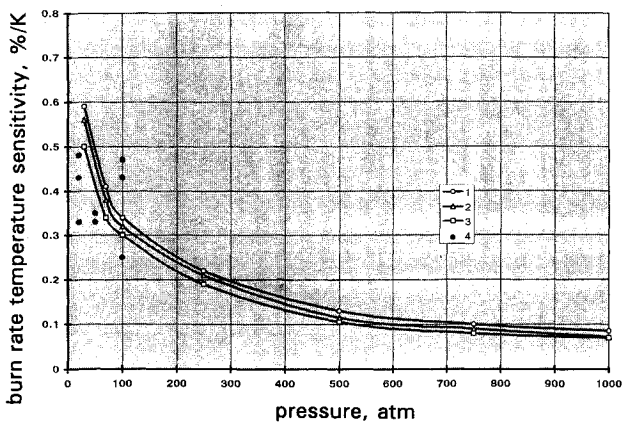

Fig. 9 Dependencies of burning rate thermal sensitivity $\beta = (\partial \ln m/\partial T_0)_p$ on pressure p: calculations by Eq. (9) (1: Q_v = 600, 2: Q_v = 800, and 3: Q_v = 1180 cal/g) and experimental point for simple DBP (points no. 4), T_0 = 20°C.

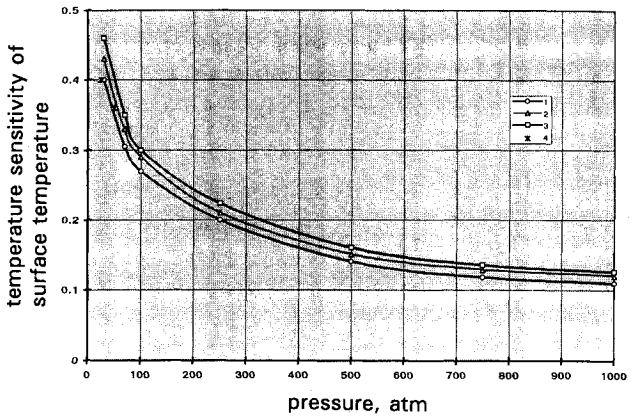

Fig. 10 Dependencies of burning surface temperature thermal sensitivity $r = (\partial T_s/\partial T_0)_p$ on pressure p: calculation by Eq. (10) (1: Q_v = 600, 2: Q_v = 800, and 3: Q_v = 1180 cal/g) and experimental points for simple DBP (points no. 4), T_0 = 20°C.

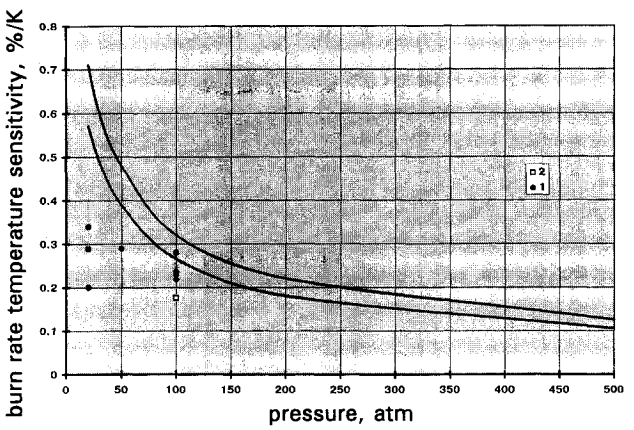

Fig. 11 Illustration of disagreement between calculation by Eq. (9) unified dependence $\beta(p)$ (u.d.) and experimental points for β of DBP with HMX. 1: DBP + 10% HMX and 2: DBP + 40% HMX.

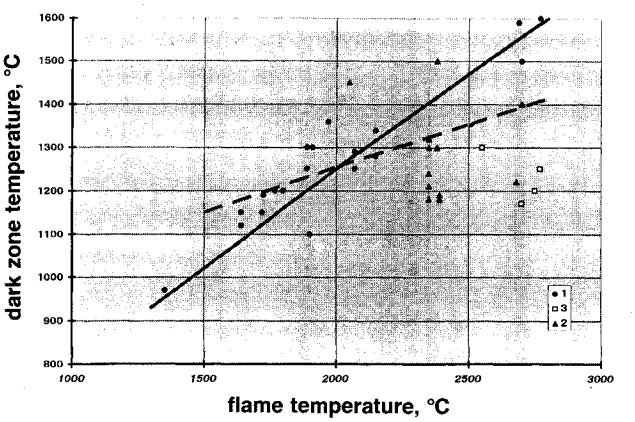

Fig. 12 Experimental dependencies of averaged dark-zone temperatures T_1 on flame temperature T_f at 20 atm, T_0 = 20°C. 1: simple DBP, 2: DBP + strong catalysts, and 3: DBP + HMX. Solid line represents averaging points no. 1, dashed line corresponds to data.[28]

Dark-Zone Laws

Two experimentally obtained characteristics of the dark zones are presented as dependencies on flame temperature T_f: 1) averaged dark-zone temperatures T_1 and 2) averaged residence times τ_r of the gas products in the dark zones.[18] The dependencies $T_1(T_f)$ for pressures of 20 and 50 atm are shown

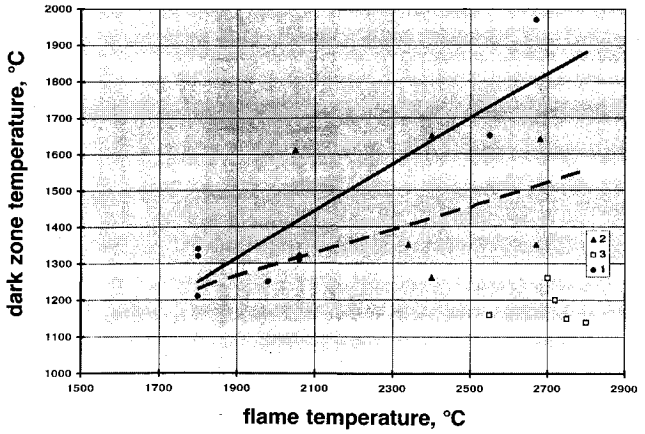

Fig. 13 Experimental dependencies of averaged dark-zone temperatures T_1 on flame temperature T_f at 50 atm, T_0 = 20°C. 1: simple DBP, 2: DBP + strong catalysts, and 3: DBP + HMX. Solid line represents averaging points no. 1, dashed line corresponds to data.[28]

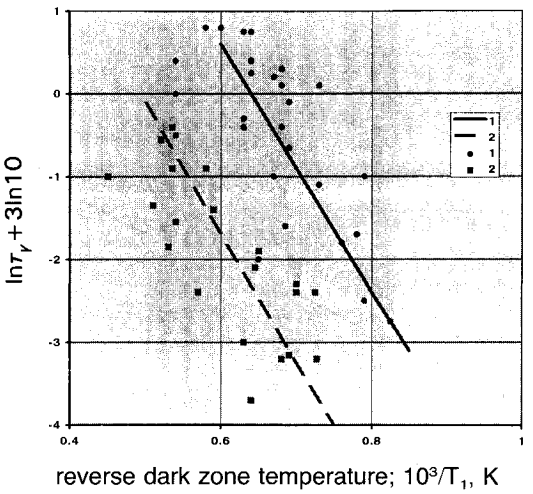

Fig. 14 Dependencies of residence time τ_r (ms) of gas products inside dark zone on reverse dark-zone temperature $(T_1, \text{K})^{-1}$ at 20 atm (1) and 50 atm (2) for DBP all types.

in Figs. 12 and 13. The scattering of the experimental points is a characteristic feature of the dark zone. Solid lines represent approximations for simple DBP, and dashed lines represent approximations for all of the propellants. The dashed lines are also in good agreement with the data indicated in Ref. 11.

Unified dependence of the function $T_1(p, T_f)$ for simple DBP can be described by the expression:

$$T_1(p, T_f) = 0.1566 \times T_f \times p^{0.350} + 645 \times \exp(-0.03p) \quad (12)$$

where p is in atm and T is in °C.

Figure 14 shows the experimental dependencies of $\tau_r(T_1)$ at pressures 20 and 50 atm for all of the propellants. Unified dependence for $\tau_r(p, T_1)$ can be described by the expression:

$$\tau_r(p, T_1) = 10^{7.2} \times p^{-2.4} \times \exp(-30{,}000/RT_1) \quad (13)$$

where τ_r has the unit of ms and T_1 of K. Dark-zone length L can be evaluated by the formula $L = m\tau_r/\rho_g$, where ρ_g is the gas density at T_1.

Chemical Interaction Between Zones of Combustion Waves of Solids

Previous works of the author[17,19] showed that heat interaction between the reaction layer of the condensed phase and hot portions of the gas phase is very slight because the distances between the burning surface and the hot flame position (or the position of the beginning of the first flame) are much larger than conductive size $k_1/c_p m$. These large distances create a large heat resistance that prevents any significant heat influence from the hot flame (or the beginning of the first flame) on the burning surface and, consequently, on the burn rate. The controlling regions of the combustion wave are the burning surface and the low-temperature portion of the gas phase near the surface.

However, dependencies (5), (8), (9), and (12) show that interactions between parameters m and T_f, T_1 do exist. Indeed, these dependencies allow us to obtain the following order of relationships:

$$m \sim T_s \sim Q \sim Q_v \quad \text{and} \quad T_1 \sim T_f \sim Q_v$$

Because this implies that propellant caloric power Q_v (heat of explosion at constant volume) links all the parameters of the combustion wave, correlations between m and T_f, T_1 are quite possible. The indicated phenomenon points to the existence of chemical interaction between zones. The nature of this interaction lies in the fact that the content of the gas phase and its temperatures (T_1, T_f) are determined by the gasification process in the burning surface.

Conclusions

The study of the mechanism of combustion was carried out for cyclic nitramines HMX and RDX and for double-base propellants containing HMX and various catalysts. Temperature distributions in combustion waves and burn-surface temperatures were obtained experimentally for HMX and RDX at pressures 1-70 (90) atm. Heat release in solid, heat feedback from gas to solid, heat-release rate in gas near the surface, and thicknesses of heat and melted layers in solid were obtained from the measurements. The data received for HMX and RDX show that values of heat release in solid are negative at low pressures (up to about 5–10 atm) and positive at elevated pressures. The heat release increases from negative values to positive values gradually, suggesting the existence of two competing processes in the reaction layer. Evaporation has a dominant role in the gasification of nitramines at low pressures, and thermal decomposition (with positive heat-release) plays the crucial role at elevated pressures. Gas-phase reaction rates near the surface of RDX are about two times greater than those of HMX; the rates increase very quickly when the pressure increases. Effective activation energies for HMX and RDX gasifications in combustion waves are equal to (46 ± 2) kcal/mole and (40 ± 4) kcal/mole, respectively. The values are in agreement with the data obtained by other methods.

The effect of cyclic nitramines on the combustion mechanism of modern double-base propellants was investigated by analyzing how the main burn-wave parameters of the propellants change when HMX is added. The empirical unified dependencies for wave parameters of simple double-base propellants (which were established in previous works), were used for analysis of the HMX influence on the propellant combustion mechanism. It has been established that the first unified law, the gasification law, which connects burning rates of propellants with burning surface temperatures, does not change significantly when HMX and catalysts are added. It implies that combustion of complex DBPs containing HMX is controlled by the DB-components (mainly by nitrocellulose). It also implies that the HMX gasification mechanism changes inside the combustion waves of complex DB-propellants because HMX and DB components have quite different macrokinetics [effective activation energy of simple DBP is equal to (21 ± 1) kcal/mole] and surface temperatures at corresponding pressures (HMX and RDX surface temperatures) are as a rule greater than those of DBP. Most of the HMX evaporates inside combustion waves of complex DBP

at all investigated pressures. This mechanism is called the "evaporation-reinforced." The increased part of HMX evaporation in combustion waves of complex DBP implies that heat release in solid of these propellants must be decreased. Experimental measurements confirm our hypothesis.

The second unified law, the heat-release law in solid that connects heat release in solid with pressure, burn rate and propellant caloric power, also does not change significantly if HMX is added (within the scatter of experimental points). It implies that the main combustion wave parameters of the complex DBP with nitramines can be estimated by referring only to the external parameters (burn rate, pressure, and propellant caloric power) for many combustion regimes. The other possibility of using the unified laws to obtain temperature sensitivities of burn rate and surface temperature (corresponding analytical formulas have been included in the article) can be realized only for the simple DBP. For nitramine-containing DBP, there are discrepancies between experimental and estimated values of the burn-rate sensitivity. As a rule, experimental temperature sensitivities are less than those estimated. The reason for the discrepancies lies in the limited validity of the unified dependencies on propellant initial temperature for nitramine-containing propellants. More exact dependencies must be established in the future.

Dark-zone laws established for simple DBP allow us to predict the temperatures and lengths of dark zones for many propellants. Nitramine (HMX)-containing propellants have decreased dark-zone temperatures in comparison with simple DBP.

The application of the dependencies has shown that burn rate and flame temperature are connected through the caloric power of the propellant. The connection can be attributed to the fact that the gasification process on the burning surface determines the composition of the gas phase and flame temperature. The connection is called "chemical interaction."

The microthermocouple technique allowed us to obtain detailed information concerning the thermal structure of combustion waves of reactive substances of different compositions. The principal characteristics of the processes that take place in zones of combustion waves have been obtained from this information. Application of the unified dependencies in the next stage of analysis will provide deeper insight into the physics of the combustion of complex substances.

Acknowledgments

This work was supported by the Russian Foundation of Fundamental Investigations, Grant 93-02-14554 and by the International Science Foundation, Grant MSP000. The author is indebted to L. DeLuca and L. Galfetti for helpful discussions.

References

[1]Boggs, T. L., *The Thermal Behavior of Cyclotrimethylenetrinitramine (RDX) and Cyclotetramethylenetetranitramine (HMX)*, edited by K. K. Kuo and M. Summerfield, Vol. 90, Progress in Astronautics and Aeronautics, AIAA, New York, 1984, pp. 121–125.

[2]Yano, Y., and Kubota, N., "Combustion of HMX-CMDB Propellants," *Propellants, Explosives, and Pyrotechnics*, Vol. 10, No. 6, 1985, pp. 192–196.

[3]Holy, J. A., "Burn Rates of Explosives at High Pressures," *Proceedings of the Conference on Compatibility of Plastics and Other Materials with Explosives, Propellants, Pyrotechnics and Processing of Explosives Propellants and Ingredients*, American Defense Preparedness Association, SC, 1985.

[4]Fifer, R. A., *Chemistry of Nitrate Esters and Nitramine Propellants in Fundamentals of Solid-Propellant Combustion*, edited by K. K. Kuo and M. Summerfield, Vol. 90, Progress in Astronautics and Aeronautics, AIAA, New York, 1984, pp. 177–219.

[5]Beckstead, M. W., and McCarty, K. P., "Modeling Calculations for HMX Propellants," *AIAA Journal*, Vol. 20, 1980, p. 106.

[6]Kubota, N., "Physicochemical Processes of HMX Propellant Combustion," *Nineteenth Symposium (International) on Combustion*, The Combustion Inst., Pittsburgh, PA, 1982, pp. 777–785.

[7]Fong, C. W., and Smith, R. F., "The Effect of Binder, Particle Size and Catalyst on the Burning Rates of PETN and RDX Composite Propellants," *Combustion Sciences and Technology*, Vol. 57, No. 1, 1988, pp. 1–15.

[8]Zhao, B.-C., and Zhao, Z.-J., "High Pressure Combustion Characteristics of RDX Based Propellants," *Twenty-Second Symposium (International) on Combustion*, The Combustion Inst., Pittsburgh, PA, 1988, pp. 1835–1842.

[9]Kuwahara, T., and Kubota, N., "Combustion of RDX/AP Composite Propellants at Low Pressures," *Journal of Spacecraft and Rockets*, Vol. 21, No. 5, 1984, pp. 502–507.

[10]Cohen, N. S., and Price, C. F., "Combustion of Nitramine Composite Propellants," AIAA Paper 81-1582, 1981.

[11]Beckstead, M. W., "Modeling AN, AP, HMX, and Double Base Monopropellants," *26th JANNAF Combustion Meeting*, Vol. IV, CPIA 526, 1989, pp. 255–268.

[12]Puchkov, V. M., and Zenin, A. A., "Thermal Structure of HMX Steady Combustion Waves," *Twenty-Fifth (International) Symposium on Combustion, Proceedings of Work-in-Progress Posters*, The Combustion Inst., Pittsburgh, PA, 1994, p. 326.

[13]Zenin, A. A., Puchkov, V. M., and Finjakov, S. V., "Investigations of Physics of Combustion of Cyclic Nitramines," *Fizika Gorenia i Vzriva* (to be submitted).

[14]Raman, K. V., and Singh, H., "Ballistic Modification of RDX-Based CMDB Propellants," *Propellants, Explosives, Pyrotechnics*, Vol. 13, No. 5, 1988, pp. 149–151.

[15]Zenin, A. A., Finjakov, S. V., Puchkov, V. M., Ibragimov, N. G., and Okrimenko, E. F., "Influence of HMX on the Mechanism of Double Base Propellant Combustion," *Fizika Gorenia i Vzriva* (to be submitted).

[16]Zenin, A. A., Finjakov, S. V., Ibragimov, N. G., and Afiatullov, E. K., "About Mechanism of Catalytic Actions in Combustion Waves of Modern Double Base Propellants," *Fizika Gorenia i Vzriva* (to be submitted).

[17]Zenin, A. A., "Thermophysics of Stable Combustion Waves of Solid Propellants," *Nonsteady Burning and Combustion Stability of Solid Propellants*, edited by L. DeLuca, E. W. Price, and M. Summerfield, Vol. 143, Progress in Astronautics and Aeronautics, AIAA, Washington, DC, 1992, pp. 197–231, Chap. 6.

[18]Zenin, A. A., and Finjakov, S. V., "Unified Dependencies for Dark Zone of Combustion Waves of Complex Nitrate Ethers," *Twenty-Fifth (International) Symposium on Combustion, Proceedings of Work-in-Progress Posters*, The Combustion Inst., Pittsburgh, PA, 1994, p. 437.

[19]Zenin, A. A., "Experimental Investigation of the Burning Mechanism of Solid Propellants and Movement of Burning Products," Ph.D. Dissertation, Inst. of Chemical Physics, Russian Academy of Sciences, Moscow, 1976 (in Russian).

[20]Klein, R., Mentser, M., Elbe, G., and Lewis, B., "Determination of the Thermal Structure of Combustion Wave by Fine Thermocouples," *Journal of Physical Chemistry*, Vol. 54, No. 4, 1950, pp. 877–884.

[21]Heller, C. A., and Gordon, A. A., "Structure of the Gas Phase Combustion Region of a Solid Double Base Propellant," *Journal of Physical Chemistry*, Vol. 59, No. 8, 1955, pp. 773–777.

[22]Zenin, A. A., "About Heat Exchange of Thermocouples in Conditions of Solid Combustion," *Journal of Applied Mechanics and Technical Physics*, No. 5, 1963, pp. 125–131 (in Russian).

[23]Zenin, A. A., "About Errors of Thermocouples Measurements Inside Flames," *Ingenerno-Physicheskij Zhurnal*, Vol. 5, No. 5, 1962, pp. 67–74 (in Russian).

[24]Zenin, A. A., "The Temperature Distribution Structure in the Steady Burning of Double-Base Propellants," *Fizika Gorenia i Vzriva*, Vol. 2, No. 3, 1966, pp. 67–76 (in Russian).

[25]Leipunskij, O. I., Novozhilov, B. V., Zenin, A. A., Ermakova, E. A., and Finjakov, S. V., "A Determination of the Function of Heat Release Rate Φ by a Given Temperature Profile T(x)," Rept. of the Inst. of Chemical Physics, Moscow, 1984 (in Russian).

[26]Zenin, A. A., "Universal Dependence for the Heat Release in Condensed Phase and Macrokinetics of the Gas Phase in the Burning Wave of Double-Base Propellants," *Fizika Gorenia i Vzriva*, Vol. 19, No. 4, 1983, pp. 78–81 (in Russian).

[27]Zenin, A. A., and Finjakov, S. V., "Unified Dependencies for Temperature Sensitivities of Combustion Rate and of Surface Temperature of Double-Base Propellants," *Proceedings of Zel'dovich Memorial Conference*, Moscow, 1994, pp. 146–148.

[28]Beckstead, M. W., "A Model for Composite Modified Double Base Propellant Combustion," *26th JANNAF Combustion Meeting*, Vol. IV, CPIA 529, 1989, pp. 239–254.